



# Plant-microbe interactions implicated in the production of camptothecin – An anticancer biometabolite from *Phyllosticta elongata* MH458897 a novel endophytic strain isolated from medicinal plant of Western Ghats of India

Madhankumar Dhakshinamoorthy<sup>a</sup>, Senthil Kumar Ponnusamy<sup>b</sup>,  
Udaya Prakash Nyayiru Kannaian<sup>c</sup>, Bhuvanewari Srinivasan<sup>d</sup>, Sripriya Nannu Shankar<sup>e</sup>,  
Kannan Kilavan Packiam<sup>a,\*</sup>

<sup>a</sup> Endophytic Fungal Metabolite Research Laboratory, Bannari Amman Institute of Technology, Sathyamangalam, Erode District, Tamil Nadu, India

<sup>b</sup> Department of Chemical Engineering, Sri Sivasubramaniya Nadar College of Engineering, Kalavakkam, Chennai, 603 110, India

<sup>c</sup> Department of Biotechnology, School of Life Sciences, Vels University, Pallavaram, Chennai, TamilNadu, India

<sup>d</sup> Department of Botany, Bharathi Women's College, Chennai, TamilNadu, India

<sup>e</sup> Marina Labs Research and Development, NT Patel Road, Nerukundram, Chennai, TamilNadu, India

## ARTICLE INFO

### Keywords:

Camptothecin  
*Phyllosticta elongata*  
Anti-cancer  
Optimization  
MTT cytotoxicity assay

## ABSTRACT

Endophytic wild fungal strain *Phyllosticta elongata* MH458897 isolated from medicinal plant *Cipadessa baccifera* from the Western Ghats region of Sathyamangalam Tiger Reserve Forest. This endophytic fungus has potential of effective anticancer drug Camptothecin (CPT). Endophytic fungi act as key symbionts in-between plants and ecosystem in the biosphere. This recently identified microbial population inside the plants produces many defence metabolites against plant pathogens. Among these defense metabolites, CPT gained much attention because of its effective anticancer activity. The maximum yield of CPT produced by optimizing the various factors like DEKM07 medium, pH 5.6, incubation time using Response Surface Methodology based on Central Composite Design. Extracted CPT is characterized using High Performance Liquid Chromatography and Electro-spray ionization-Mass spectrometry. The highest yield of CPT was 0.747 mg/L was produced at optimized factors of dextrose – 50 g L<sup>-1</sup>, peptone – 5.708 g L<sup>-1</sup>, magnesium sulphate – 0.593 g L<sup>-1</sup>, and incubation time – 14 days. *In-vitro* MTT assay revealed the CPT derivatives were cytotoxic to A-549 cancer cell line (IC<sub>50</sub> 58.28 µg/ml) as nearly compared to the (IC<sub>50</sub> 51.08 µg/ml) standard CPT. CPT producing strain *P. elongata* from *C. baccifera* has the potential of CPT biosynthesis, and could be an effective anticancer bio metabolite. This compound has been described in the literature to be an effective anticancer metabolite. Our findings support the novel lifesaving anticancer drug from endophytic fungus in forest ecosystem concludes effective utilization of key symbionts will safeguard the humans and forest ecosystem.

## 1. Introduction

Cancer is the leading cause of death worldwide and is increasing every day. There were an estimated 9.6 million deaths in 2018 due to cancer reported by the World Health Organization (WHO). Exposure of various chemicals like Dichloro-diphenyl-trichloroethane (DDT), Dioxins and trihalomethane are highly associated with cancer (Rodgers et al., 2018; Téllez Tovar and Rodríguez Susa, 2020). The previous

GLOBOCAN - 2018 report estimated that all groups of individuals affected by 36 new types of cancer had a high mortality rate (Bray et al., 2018). Of the various types of cancer, lung cancer (18.4%) and breast cancer (11.6%) are most commonly diagnosed in males and females, respectively followed by colorectal cancer (10.2%) throughout the world (Bray et al., 2018). Various researchers have reported the potential activity of endophyte anticancer bioactive metabolites such as Taxol, CPT, Podophyllotoxin and Vinblastine (Subban et al., 2019;

\* Corresponding author. Endophytic Fungal Metabolite Research Laboratory, Department of Biotechnology, Bannari Amman Institute of Technology, Sathyamangalam, Erode District, Tamil Nadu, India.

E-mail addresses: [dhakshnamadhananj89@gmail.com](mailto:dhakshnamadhananj89@gmail.com) (M. Dhakshinamoorthy), [senthilkumarp@ssn.edu.in](mailto:senthilkumarp@ssn.edu.in) (S.K. Ponnusamy), [nkudayaprakash@gmail.com](mailto:nkudayaprakash@gmail.com) (U.P. Nyayiru Kannaian), [drsbhuvanewari8@gmail.com](mailto:drsbhuvanewari8@gmail.com) (B. Srinivasan), [nsripriya.bt@gmail.com](mailto:nsripriya.bt@gmail.com) (S.N. Shankar), [drkpkannan@gmail.com](mailto:drkpkannan@gmail.com) (K. Kilavan Packiam).

<https://doi.org/10.1016/j.envres.2021.111564>

Received 27 April 2021; Received in revised form 28 May 2021; Accepted 12 June 2021

Available online 3 July 2021

0013-9351/© 2021 Elsevier Inc. All rights reserved.

Venugopalan and Srivastava, 2015). CPT is a plant-derived quinoline alkaloid which inhibits topoisomerase – I (hTop1) in tumour cells. CPT binds to the active site of tyrosine (Tyr723) in the process of replicating hTop1 DNA and slows down cytotoxic effects in humans (Pommier, 2006). Another benefit of the CPT is the formation of the  $1\alpha$  factor induced by hypoxia (HIF1 $\alpha$ ). CPT and its formation of a blocking ribosome that leads to inhibition of translational response (Hertzberg et al., 1989; Jiang et al., 2018). Scientists believe that CPT derivatives of topotecan, irinotecan and doxorubicin may be used to treat cancer cell lines in the lungs and ovaries (Chen et al., 2020).

The annual demand for CPT has been reported to 3000 kgs in the international market, but the annual production of CPT is only about 1/6th of the global market demand (Nat et al., 2015). Currently, a significant amount is provided through the use of herbal medicines as a source material (Yang et al., 2017). But as a result of environmental concerns and huge demand, an alternative source must be identified and studied for sustainable production. Consequently, in vitro production of CPT from endophytes could be a potential alternative; it is beneficial to produce at low cost without affecting the ecological system (Kai et al., 2015; Shweta et al., 2013; Venugopalan et al., 2016). (Puri et al., 2005) published the first report on CPT production from endophytic fungi *Nothapodytes foetida*. Endophytes have been identified from all parts of plants belonging to a different species (Busby et al., 2016). Around 80,000 endophytic fungal species have been reported globally, and only 60% of them have been identified to date, and the rest has not been identified yet. Few of the industrially important asexual forms of fungi were reported (Nomila Merlin et al., 2013; Venugopalan and Srivastava, 2015) and these forms of medicinal fungi can produce highly valuable metabolites within the plants because of the symbiotic association. Deuteromycete medicinal fungi are not much involved in primary metabolism, and they can produce secondary metabolites for fungal growth and also at the host because of influencing ecological imbalance. They act as signaling molecules and support the environmental niche (Calvo et al., 2002).

Several recent research articles (Kathiravan and Raman, 2010; Subban et al., 2019) have reported the potential anticancer compounds of Taxol from coelomycetes. Vinblastine has been isolated in coelomycetes endophytic fungi of *Phyllosticta* sp., *Pestalotiopsis* sp., *Botryodiplodia* sp., and *Colletotrichum* sp. Various reports of CPT from endophytic fungi belong to Hyphomycetes and Ascomycetes were recorded with the methodology and yield variation (Musavi and Balakrishnan, 2014; Shweta et al., 2013). To date, there are no published data about the production of CPT using endophytic fungi isolated from medicinal plants used by the tribal people living in the forest region, Thalamalai range (STRF). In this present study, the coelomycetes endophytic fungi were investigated and isolated from host medicinal plants for the production of anticancer drug (CPT) under in-vitro condition. The study also covers the optimization of the media components and the fermentation conditions using Response Surface Methodology (RSM) based on Central Composite Design (CCD) is used to find the mutual interaction effects between the variables in any fermentation process (Bhalkar et al., 2016; Clarence et al., 2019). This study will address the fact that the potential strains isolated from the forest of the Sathyamangalam Tiger Reserve have huge potential to use it as a source of CPT production.

## 2. Materials and methods

### 2.1. Screening of camptothecin producing endophytic fungal culture

#### 2.1.1. Study area description and collection of medicinal plant samples

The Study area, Sathyamangalam Tiger Reserve Forest (STRF) is present in the Nilgiris Biosphere Reserve, an important wildlife corridor linking the Western Ghats with the Eastern Ghats located in the adjoining states of Tamil Nadu and Karnataka, India. The STRF is represented by various types of forest types such as tropical dry deciduous, tropical scrub, tropical moist deciduous, tropical semi-evergreen forests

etc. The STRF is categorized and administered by seven distinct ranges, Bhavani Sagar, Germalam, Hasanur, Sathyamangalam, Thalamalai, TN Palayam and Thalawadi by forest authorities. The study area is very rich in wildlife and is home to a large population of Asian elephants, tigers and many other wild animal and plant species. The mean temperature of the study area is 21.54 °C and 32.84 °C, and the mean annual rainfall is 824 mm. The sample collection was carried out from the Kaalithimbam – Ittarai forest, Bejalatti beat of Thalamalai Range, STRF, Tamil Nadu, India, latitude and longitude of 11.58499° N – 77.07175° E covering 1411 sq. km and situated 1281 m above sea level. The medicinal plant of *Cipadessa baccifera* (Roth) Miq. Commonly referred to as “Pulichorai” in the local language of Kannada and Tamil. The Camptothecin (CPT) producing fungal strains is isolated from *C. baccifera*. Field trips were performed periodically, and the plant sample was safely collected and transferred to sterile bags and stored in the laboratory at a temperature of 4 °C further use.

#### 2.1.2. Isolation, molecular identification of endophytic fungi

The methodology of the surface sterilization protocol is briefly explained (Dhakshinamoorthy et al., 2021). It was used to isolate the endophytic fungi from the leaves of a plant under laboratory conditions and blot dry. The leaves were cross segmented 0.5 × 0.5 cm and placed into Potato Dextrose Agar plates amended with Streptomycin (100 µg/ml) and incubated at 26 ± 2 °C for 4 weeks in a light chamber. Emerging fungal cultures were sub-cultured, identified, and stored at 4 °C for further CPT screening. Morphological and microscopic characteristics of endophytic fungi were identified based on the standard manuals (Nagraj et al., 1972; Sutton, 1980). Photomicrographs were taken under light microscopy (Olympus CX31, Canon EOS 700D series, China) at the magnification of 100×. Identified cultures of endophytic fungi were deposited with the Endophytic Fungal Metabolites Research Laboratory, Department of Biotechnology, Bannari Amman Institute of Technology, Sathyamangalam, Erode District, India. The CPT producing endophytic fungal strain was identified by selecting ITS primers ITS1, and ITS4 conserved regions of 18S rDNA genes to amplify the different loci of internal transcribed regions, and the retrieved sequence was submitted to the NCBI gene BankIT. The search for similarity gene sequences was carried out with the help of the basic local alignment search tool (BLAST). The endophytic fungal gene sequence with a homology score greater than 97% was assigned to the same phylotype. The phylogenetic tree was constructed using Molecular Evolutionary Genetics Analysis (MEGA) version X and the National Centre for Biotechnology Information (NCBI) from the homology scores of the BLAST results. Maximum composite likelihood method was used to compute the evolutionary distance (Kumar et al., 2018). The evolutionary relationship of the endophytic fungal taxa was inferred using the Neighbor Joining method, and the bootstrap consensus tree was deduced from 500 replicates.

#### 2.1.3. Screening of CPT producing endophytic fungi

Different media were prepared based on previous CPT literatures of endophytes (Clarane et al., 2019; Pu et al., 2013). Six liquid media, including DEKM07 medium (consists of Potato extract (peeled and diced) 250.0 g L<sup>-1</sup>, Dextrose 20.0 g L<sup>-1</sup>, Peptone 10.0 g L<sup>-1</sup>, MgSO<sub>4</sub>.7H<sub>2</sub>O 0.5 g L<sup>-1</sup>; pH 5.6), Potato Carrot Broth (PCB) medium (Potato extract 250.0 g L<sup>-1</sup>, Carrot 20.0 g L<sup>-1</sup>, pH 6.7), Sabouraud Potato Dextrose (SPDB) modified medium (Potato extract 250.0 g L<sup>-1</sup>, Dextrose 20.0 g L<sup>-1</sup>, Tryptone 10.0 g L<sup>-1</sup>, pH 5.2), and Potato Dextrose Broth (PDB) (Potato extract 250.0 g L<sup>-1</sup>, Dextrose 20.0 g L<sup>-1</sup>; pH 5.6), Malt extract (ME) medium (Malt extract 20.0 g L<sup>-1</sup>, Dextrose 20.0 g L<sup>-1</sup>, Peptone 6.0 g L<sup>-1</sup>; pH 5.9), and Czapek Dox (CZD) medium (Dextrose 30.0 g L<sup>-1</sup>, NaNO<sub>3</sub> 3.0 g L<sup>-1</sup>, KH<sub>2</sub>PO<sub>4</sub> 1.0 g L<sup>-1</sup>, KCl 0.5 g L<sup>-1</sup>, MgSO<sub>4</sub>.7H<sub>2</sub>O 0.5 g L<sup>-1</sup>, FeSO<sub>4</sub>.7H<sub>2</sub>O 0.01 g L<sup>-1</sup>; pH were adjusted to 5.5), suspension culture of 50 ml medium was prepared each in 250 ml Erlenmeyer flask and mass culture was incubated at 27 °C in a rotating shaker at 120 rpm for a period of 12 days. CPT producing cultures were

extracted and screened through UV–Visible spectrophotometer and Thin Layer Chromatography. The small amount of fungal crude from each medium was dissolved in  $\text{CHCl}_3$  and subjected to UV and thin layer chromatography on silica gel - G (0.5 mm thickness) using  $\text{CHCl}_3$  – MeOH (4:1 v/v) as the solvent system for the confirmation of CPT production. All the experiments were carried out in triplicate.

## 2.2. Extraction of camptothecin

Section 2.1.3. explains the best producing fungal isolate obtained from the protocol. The CPT producing fungus was harvested at the DEKM07 medium with process conditions of temperature (27 °C), agitation speed (150 rpm), pH (5.6), was maintained based on previous studies (Pu et al., 2013; Venugopalan and Srivastava, 2015) for the estimation of biomass (g/l) and CPT yield (mg/g of dry weight). The endophytic fungal culture was centrifuged at 10,000 rpm, 4 °C for 15 min, and the pellet was washed thoroughly with sterile distilled water to remove the hydrophilic compounds. To the supernatant, an equal volume of chloroform ( $\text{CHCl}_3$ ): methanol (MeOH) (4:1 v/v) mixture was added and ultrasonication was then performed twice at 50% frequency, 33 KHz for 5 min. The upper alkaloid layer was collected at each cycle, and an equal volume of pellets in grams,  $\text{CHCl}_3$  – MeOH (4:1 v/v) were added. This process was repeated thrice to collect fungal alkaloid metabolites in a separating funnel, and the upper layer was separated. Using rotary evaporator, the crude was concentrated at the pressure of 10 psi and a temperature of 40 °C. The crude extract was filtered using a syringe filter (0.2  $\mu\text{m}$ ), and the filtrate was maintained at 4 °C until further analysis. The crude filtrate was redissolved in  $\text{CHCl}_3$  – MeOH (4:1 v/v) for the further analysis of CPT (Pu et al., 2013). method was applied to characterize the secondary metabolite from crude fungal extract with standard CPT (purchased from Sigma Aldrich).

## 2.3. Characterization and quantification of camptothecin derivatives

The mixture of compounds was separated in HPLC (Agilent 1220 Infinity series - Agilent Technologies, California, USA), binary gradient system with analytical separation was performed using a zorbax SB – C18 column (internal diameter, 2 mm; length, 150 mm; particle size, 3  $\mu\text{m}$ ) and a guard column (Phenomenex, Torrance, CA) at a flow rate of 200  $\mu\text{l min}^{-1}$  at 30 °C. The 10  $\mu\text{l}$  of the sample dissolved in  $\text{CHCl}_3$  – MeOH (4:1) was injected. The mobile phase of water (A) and acetonitrile (B) was used in the ratio of 25:75, and the UV detector was recorded at  $\lambda_{\text{max}}$  365 nm. Quantification of CPT analysis was carried out to determine the wavelength of standard CPT that was submitted to HPLC analysis. The determination of CPT analysis was followed by the methodology of (Pu et al., 2013). The stock solution of standard 1 mg CPT was prepared in the solvent mixture of  $\text{CHCl}_3$  – MeOH in the ratio of 4:1. Further, dilutions were made using the stock solution to prepare different concentrations of CPT. The standard CPT calibration curves was estimated at the wavelength of 365 nm and the fungal CPT was determined by using the regression equation (Eq. (1)).

$$y = 5379.2x + 3754.4 \quad (1)$$

The extracted compounds were analyzed using FTIR spectroscopy (Shimadzu, IR affinity, Japan) for the detection of single functional groups and different lateral chains as well as hydrogen bonds. Detection of functional group was recorded within the wave number range of 4000–500  $\text{cm}^{-1}$ . CPT and its derivatives were determined using electron spray ionization mass spectrometry (Micromass QuattroII Triple Quadrupole Mass Spectrometer, United States). The spectrum was collected in 5 s scans with the operating conditions of the sample flow rate 5  $\mu\text{L/min}$ , capillary cone voltage 40 V, source temperature 120 °C, desolvation temperature 300 °C, and positive ionization mode. The CPT and its derivatives were identified based on previous publications in PubChem databases.

## 2.4. Determination of mitochondrial synthesis by MTT assay

In order to determine the cytotoxicity effect, the viability was monitored with different concentrations of fungal CPT extract and standard CPT against human lung cancer carcinoma – A 549 monolayer cell culture using 3-(4,5-Dimethylthiazol-2-yl) – 2,5-diphenyltetrazolium bromide assay. The cell culture was trypsinised and maintained in DMEM with 10% bovine fetal serum. 100  $\mu\text{l}$  of diluted cell suspension was added in 96 well micro titre plates, and the plates were then incubated at different conditions at 37 °C for 24 h and 72 h in 5%  $\text{CO}_2$  atmosphere and microscopical observations were carried out and recorded every 24 h. After 72 h, the solution sampled in the wells was released and 20  $\mu\text{l}$  of MTT (2 mg/ml) in MEM – PR (MEM free of phenol red) was added to each well. The plates were smoothly stirred and incubated for 3 h at 37 °C and a thick layer was removed and collected. To this, 50  $\mu\text{l}$  of isopropanol was added. The plates were delicately agitated to dissolve the formed formazan. Absorbance was measured using a microplate reader with a wavelength of 540 nm. The percentage of cell viability was calculated (Eq. (2)), and the concentration of drugs or test samples required to inhibit cell growth by 50% was determined from the dose-response curves of each cell line.

$$\% \text{ Cell Viability} = \frac{\text{Mean OD of individual test group}}{\text{Mean OD of the control group}} \times 100 \quad (2)$$

## 2.5. Optimization of process parameters for maximizing CPT yield

The important factors that have significant role on the production of CPT such as dextrose, peptone, magnesium sulphate, and incubation time were taken for determining the optimum levels using Response Surface Methodology (RSM).

### 2.5.1. Design of experiments and response surface methodology

Central Composite Design (CCD) model of Response Surface Methodology (RSM) was generated using STAT-EASE Design Expert 12.0. A set of 28 experimental runs was carried out to optimize the medium composition at shake flask level. The software was analyzed both estimated and actual response and formed the quadratic polynomial equation (Table 2). The equation was used to evaluate the independent variables viz., medium components and incubation time and also the interaction effect between them. The biomass and CPT production was taken as response variables and determined by (Musavi et al., 2015; Pu et al., 2013).

### 2.5.2. Medium parameters, optimization criteria, and numerical criteria

Based on previous literatures and experimental studies, parameters like dextrose, peptone, magnesium sulphate and incubation time were chosen as independent variables (Clarance et al., 2019; Musavi et al., 2015). Since they were significantly influencing the cell-associated CPT accumulation, these independent variables were chosen to perform the experiments. Each of them in this design at three different levels of (–1, 0, +1). The optimization criteria and numerical criteria are very important to increase the concentration of CPT in fungal biomass. The levels of variables ranging from dextrose 10–50  $\text{g L}^{-1}$ , peptone 1–10  $\text{g L}^{-1}$ , magnesium sulphate 0.1–0.6  $\text{g L}^{-1}$ , and incubation time 4–14 days were selected as independent variables to run the experiments. Both linear and quadratic effects and interaction between four independent variables were calculated based on biomass and CPT yield. The accuracy of the model of both linear and quadratic equations were tested in the Analysis of Variance (ANOVA), and the results were shown in (Table 3). The significant values of each coefficient were determined using F-test and p-value;  $p < 0.05$  was considered to be fit, and the model was suggested for further studies.

### 3. Results and discussion

#### 3.1. Ethno-pharmacological study on medicinal plants at Sathyamangalam Tiger Reserve (STRF)

The medicinal plant was collected from Ittarai forest, Bejalatti beat in the Thalamalai range of STR, and authenticated as *Cipadessa baccifera* (Roth) Miq. belongs to Meliaceae by Botanical Survey of India, Southern Regional Centre, Coimbatore, India (Authentication Number: BSI/SRC/5/23/2017/Tech/262/102 dated on May 05, 2017). The specimen also identified with Plant List database, International Plant Name Index (IPNI) Database and Environmental Information System (ENVIS), Government of India. The ethno-pharmacological study was carried out in different ranges of STR was represented in Table S1. In addition, plant photographs were taken to confirm the taxonomical identification. The study showed that *C. baccifera* is endemic to the Western Ghats and it is a vital source to cure many diseases like cancer, snakebites, diabetes (Ramkumar et al., 2015). (Reddy et al., 2019) reported the ethno-pharmacological studies of *C. baccifera* shrub that could be used to treat diabetes and wounds from Seshachalam biosphere of Eastern Ghats. Similar results were obtained with *C. baccifera* in different geographical regions (Ning et al., 2010a, 2010b, 2010b). (Liu et al., 2012) were reported the leaf parts were used to treat gastroenteritis, *Diabetes mellitus*, catharsis from the Wuliang mountains of China. Further, CPT was first to isolate from the endophytic fungi of *C. baccifera* from Sathyamangalam Tiger Reserve Forest.

#### 3.2. Isolation, screening, and identification of endophytic fungi

Based on the ethno-pharmacological studies, the medicinal plant *C. baccifera* was selected for the isolation of endophytic fungi for a screening of CPT. The endophytic fungal isolation study was carried out in PDA Petri-dishes for 2–4 weeks, and the emerging fungal propagules were isolated and sub-cultured for CPT screening. The endophytic fungal colonies were identified to isolate the pure colonies from colonized segments. So, these colonies were sub-cultured to get pure colonies for further studies. A total of 50 endophytic fungal isolates belonging to 8 genera and 8 sterile forms, in total 16 fungal taxa were recovered from 50 segments of plant (Table S2). The predominant endophytic fungi from leaves viz., *Phyllosticta elongata*, *Pestalotiopsis* sp., *Colletotrichum* sp., *Fusarium moniliforme*., *Phoma glomerata*, and *Chaetomium* sp., were obtained. CPT producing endophytic fungus *Phyllosticta elongata* has been identified through morphological and microscopical characteristics (Fig. 1 a, b & c) i.e., colonies reaching 3 cm dia in 10 days on PDA plate, olive-green to greenish-black when the cells get matured, olivaceous to greenish-black on the reverse. Pycnidia globose, conidiogenous cells hyaline cylindrical, single-celled, broadly ovoidal, 7–11 mm with short appendages, and the pycnidia were visible after 30 days. The morphological and microscopical characteristics as *Phyllosticta elongata* were identified through manuals for coelomycetes characterization (Nagraj., 1980; Sutton., 1984).

A total of 25 BLAST similarity sequences were selected due to 97% similarity to *Phyllosticta elongata*. Further, the sequence was submitted into (NCBI) GenBank and received accession number ID: MH458897.1.

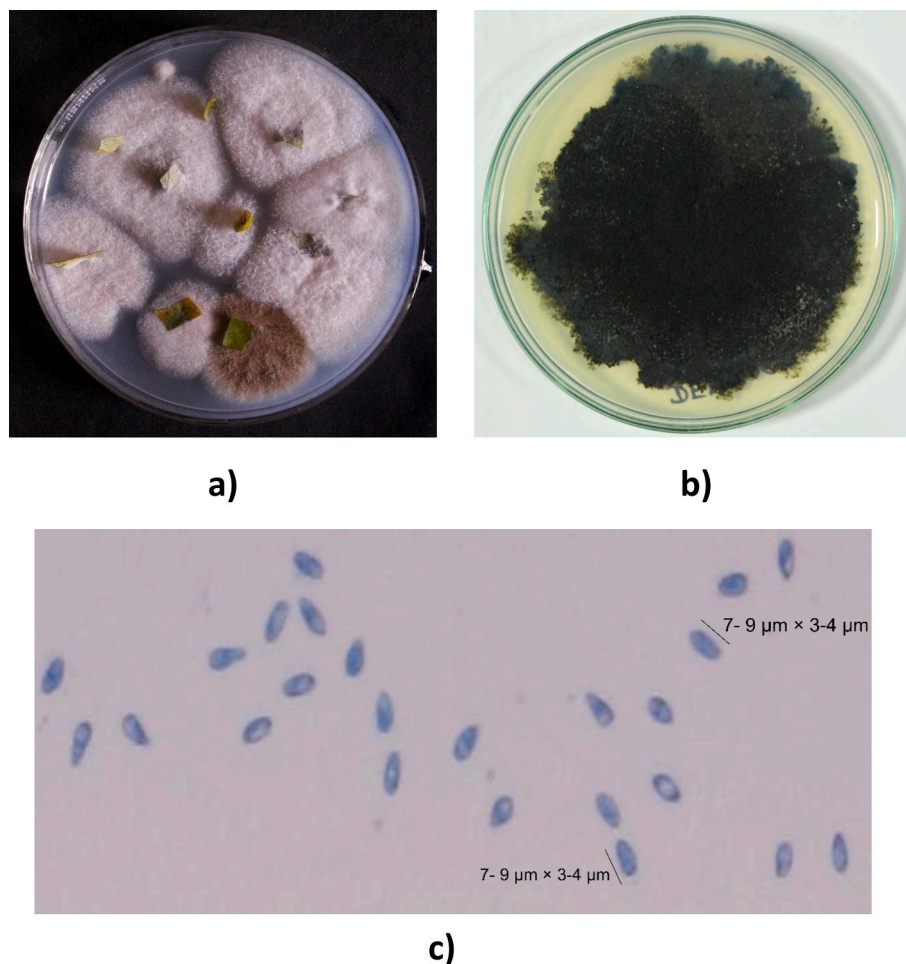


**Fig. 1.** (a–c) Isolation and identification of endophytic fungi a) Emerging fungal propagules from plant parts of *Cipadessa baccifera* b) Axenic culture of fungal colonies of *Phyllosticta elongata* c) Spores of *Phyllosticta elongata* at 100× magnification.

>AAATGACCTTCTACCCCTTGTTACTACTATGTTGCTTGGCGGGT-CGACCTGGTTCCGACCCAGGCGCGCCGCCAGCCTTAAGTGGC-CAGGACGCCCGCTAAGTGCCCGCCAGTATACAAAACCTCAA-GAATTCATTTTGTGAAGTCTGATA-TATCATTTAATTGATTAATACTTTCAA-CAACGGATCTCTTGGTTCTGGCATCGATGAA-GAACGCAGCGAAATGCGATAAGTAATGTGAATTGCA-GAATTCAGTGAATCATCGAATCTTTGAACGCA-CATTGCGCCCTCTGGTATTCCGGAGGGCATGCCTGTTCGAGCGT-CATTTCAACCCTCAAGCTCTGCTTGGTATTGGCAACGTCCGCTGCCG-GACGTGCCTTGAA-GACCTCGGCGACGGCGTCTAGCCTCGAGCGTAGTAGTAAAA-TATCTCGCTTTGGAGTGTGGGCGACGGCCGCCGAAAAATC-GACCTTCGGTCTATTTTCCAGGTTGACCTCGGATCAGGGAGGGA-TACCCGCTGAACTTAAGCATATCAATAAGC. A total of 549 base pairs were recorded; the Neighbor joining method was used to construct the phylogenetic tree (Kumar et al., 2018). Evolutionary distances were derived using the maximum composite likelihood method (Kumar and Hyde, 2004). and in the units of the number of core substitutions per site and this analysis consisted of 25 nucleotide sequences. All ambiguous positions were removed for each sequence pair (pairwise deletion option). Based on the phylogenetic tree and evolutionary analyses, *P. elongata* was confirmed through molecular level phylogenetic relationships conducted in MEGA X. Due to geographical location, seasonal changes, the plant may adapt the different endophytic fungi like *Phyllosticta* sp., *Fusarium* sp., etc.; the endophytic infection rate was 100%, respectively, in leaves (Kumar and Hyde, 2004). Earlier studies also revealed that predominant endophytic fungal diversity was high in these forest areas due to the presence of biodiversity hotspots and high fungal amplitude to the host (Govinda Rajulu et al., 2013; Reddy et al., 2016; Suryanarayanan et al., 2011). The predominant endophytic fungal colonies have the maximum symbiotic relationship with plants and produce secondary metabolites, enzymes to attain succession ecotype in a particular environment. So, the plants have a self-defense mechanism with all other toxic activity with mutualistic relation with endophytic fungi. This could be one of the advantages to screen predominant fungi from plants for secondary metabolites, especially CPT screening.

### 3.3. Selection of CPT producing endophytic fungi through the basal medium

During the study, the isolate *Phyllosticta elongata* is predominantly present in leaf segments of *Cipadessa baccifera*. This indicated that the ecological niche of a particular environment was predominantly occupied by *P. elongata* (Wikee et al., 2013; Wulandari, 2013). Previous studies also stated that endophytic fungi *Phyllosticta* species producing anticancer compounds like Taxol, Tauranin, etc., were suggested for CPT screening (Kumaran et al., 2009). The CPT producing *P. elongata*, was screened from other isolates using various basal medium. But only CPT molecules were detected in potato carrot broth (PCB) medium, sabouraud potato dextrose (SPDB) modified medium, and potato dextrose broth (PDB) (Clarance et al., 2019). No CPT was detected in malt extract (ME) medium, Czapek dox (CZD) medium and CPT production were highly obtained in DEKM07 medium by *P. elongata* (Fig. S1). The CPT and biomass growth were achieved at these optimal conditions in DEKM07 basal medium. The glucose was used as carbon source in the DEKM07 basal medium for *P. elongata* to increase the biomass and CPT concentration. Peptone, a short-chain peptide partial digested nitrogen source rich in the DEKM07 medium could easily enter into the metabolic pathway for tryptamine formation when compared with other nitrogen sources. The tryptamine is a key precursor to accumulate the CPT concentration in biomass. Glucose and peptone were entered into the cytosol to synthesize the monoterpenoid indole alkaloids from strictosidine. The strictosidine is key intermediate to regulate the pathway of isopentenyl diphosphate (IPP) and mevalonate (MVA) pathway by condensation of tryptamine with secologanin. It was

a key metabolite that has the potential to form a variety of natural products in biosynthetic pathways (Kai et al., 2015; Pu et al., 2013). Previous evidence was indicated the secologanin moiety of CPT was formed by the MVP pathway in *Catharanthus roseus* by (Wang et al., 2015). Supplemented trace elements of magnesium sulphate were added into the DEKM07 medium and are necessary for fungal growth to increase the biomass concentration (Liu et al., 2010; Musavi et al., 2015; Puri et al., 2005). These factors are crucial to develop both biomass and CPT concentration, on the other side of basal media like CDB; ME broth has the media components of NaNO<sub>3</sub>, and tryptone which did not much influence the production of secondary metabolite. The other micro supplements such as ferrous sulphate, and KH<sub>2</sub>PO<sub>4</sub>, influenced the concentration of biomass but not CPT metabolite. This might be due to symbiotic association with plants defence mechanism. The maximum mycelial growth of *P. elongata* was observed on the DEKM07 medium. The CPT metabolite production was higher in the DEKM07 medium on the complete utilization of substrate for its fungal biomass growth of 14.2 g and CPT yield was 0.694 mg/L. So, the DEKM07 medium would be the optimal easy to use in pharmaceutical industries for further CPT production at mass level at low cost.

### 3.4. Characterization of CPT

#### 3.4.1. Preliminary characterization of endogenously produced CPT

Preliminary identification of CPT was examined through UV-Visible spectrometer, and further by Thin Layer Chromatography techniques in the fungal crude extract. The maximum absorbance of UV was recorded at 365 nm, with a negligible difference in absorbance values of 0.10 between the standard and fungal samples was compared. The UV results showed that the fungal CPT absorbance rate was correlated with standard CPT and also previous reports revealed the similarity of absorbance peak at 365 nm corresponds to fungal CPT, respectively (Patil et al., 2014). Three significant fractions were recovered with that of CPT derivatives exhibiting fluorescent green colour in the silica-coated TLC plate. Rf values of standard and fungal CPT of TLC were recorded with 0.44 and 0.43, respectively. These values were compared with previous studies of CPT, and Taxol screening (Bhalkar et al., 2016; Kathiravan and Sri Raman, 2010).

#### 3.4.2. HPLC analysis

An attempt was made to characterize and quantify the CPT derivatives present in the fungal crude extract. The fungal crude extract of *Phyllosticta elongata* was analyzed by using RP-HPLC. Stock solutions were prepared to compare the calibration curve. Based on this, HPLC was performed to quantify the CPT of 0.694 mg/L. Similar results were obtained with CPT by (Amna et al., 2012). The fungal CPT peak was eluted at a retention time of 6.044 min. When compared with the retention time of standard CPT at 6.047 min was observed. Similar results of HPLC fungal peak absorbance was obtained from *Xylaria* sp., and the retention time was 6.1 min (Liu et al., 2010) as the evidence of CPT. The CPT yield was 10-folds higher than the previous results of (Bhalkar et al., 2016; Shweta et al., 2013).

#### 3.4.3. Quantification of CPT

The fungal isolate *Phyllosticta elongata* were grown in DEKM07 medium and mycelial mat was harvested and analyzed at the end of 12 days period. The fungal broth did not show any CPT derivatives due to the uptake the extracellular metabolites and its secretion of secondary metabolites into intracellular cells. The *P. elongata* gained much interest in intracellular source of DEKM07 media for CPT production. The CPT and biomass were analyzed through preliminary characterization of UV visible spectrometer, Thin Layer Chromatography, and further quantified with HPLC. The fungal biomass obtained was 14.2 g L<sup>-1</sup>, and CPT yield in the biomass was estimated at 0.694 mg/L. High yielding CPT derivatives were obtained from *P. elongata* mycelial mat were higher than the reported endophyte *Fusarium solani* etc., of CPT production

were represented in Table 1. This was the first report of CPT from *Phyllosticta elongata* endophytic fungi from STRF. The results suggested that there may be other predominant endophytes in host plants in particular geographical indicated regions of the Western Ghats that have the potential to produce secondary metabolites. The study area clearly indicates the biodiversity hotspot and maintains the plant-endophyte symbiotic adaptations to produce CPT for self defence mechanism against other ecological niches as it was compared with other metabolites like Taxol, Doxorubicin from Western Ghats (Reddy et al., 2016; Subban et al., 2019). The fungal CPT was further analyzed and identified with FTIR and ESI-MS analysis for in-vitro toxicity MTT assay.

#### 3.4.4. Fourier transform infra-red spectroscopy analysis

FT-IR spectra have been recorded in this study indicates that intense vibrations in experimental analysis with a comparison of the standard CPT spectrum. In this study, off-plane flexion vibration C-H=CH<sub>2</sub> was observed in the 949.98 cm<sup>-1</sup> area and is generally very strong. Out-of-plane C-H bending modes are typically lower in the 600–950 cm<sup>-1</sup> region. The IR spectrum showed that 1067.65 cm<sup>-1</sup> corresponded to C-H vibrations; the deflection of the C-H plane for an average intensity and recorded at 1350–950 cm<sup>-1</sup>. Carbon-carbon vibrations of the phenyl group were observed in the 1650–1200 cm<sup>-1</sup> area (Bellamy, 1975). The C-C stretching peaks appeared in the infrared spectrum were assigned to skeletal C-C bonds while the band at 1529.62 cm<sup>-1</sup> had been assigned to the ring C-N stretching vibrations. Arjunán et al. (2009) studied amino-methylquinoline under symmetry C; carbon-to-carbon stretching bands developed in the infrared spectrum. The C-C and C-H stretch vibrations determined the existence of one or more aromatic ring structures, and have been designated as C-H stretching vibrations of the quinoline ring of CPT. The presence of two C=O stretches can enhance

the unique strong vibratory binding character, resulting in bands at 1672,36 and 1689,72 cm<sup>-1</sup>. The narrow peak in the range of 1800–1600 cm<sup>-1</sup> belongs to carbonyl compounds, and the double bonds of C=O have force constants of magnitudes as compared with standard CPT of C=O stretch (Silverstein et al., 1991; Socrates, 2001). The P-H stretch with a strong intensity and average suggests the presence of phosphines, which could be derivatives of the compound. The vibrations of the methyl group were substitutes giving electrons into the aromatic cyclic system. CH<sub>3</sub> C-H anti-symmetrical stretch was found to be 2827.77 and 2966.65 cm<sup>-1</sup> (Sajan et al., 2006). The N-H section exhibits average vibrations and accurate correlations with the baseline and published CPT data (Joseph et al., 1987). The O-H peak has a narrower band and a higher intensity, indicating the implication of intra-molecular hydrogen collage. This binding results in a strong stretching vibration in the plane of the hydroxyl group observed between 3700 and 3600 cm<sup>-1</sup> (Sajan et al., 2006). The FTIR spectra was compared with the literature values (Chai et al., 2019). It was observed that the spectral bands in the FTIR analysis displayed characteristic peaks of C-C stretching peaks and C-N stretching vibrations.

#### 3.4.5. Electron spray ionization – mass spectrometry analysis

Partially purified endophytic fungal crude extract was used to analyze the CPT derivatives through the advanced analytical technique of ESI-MS analysis. The structure of compounds identified was presented in (Fig. 2), and CPT derivatives were identified as cancer curative agents through previous literatures from PubChem and Chem spider databases. ESI-MS technique allows the characterization of molecules dependent on mass with a high precision charge ratio. Nine out of twenty-one isolates were CPT and its derivatives with m/z 347.42, 348.96, 349.04, 351.33, 363.15, and 423.21, were determined and it correlates with findings of 348 and 365 MH<sup>+</sup> ions of HPLC-MS results of (Liu et al., 2010). Similar results of 349.04 m/z were obtained during CPT production when compared with 349.1204 m/z of (Bhalkar et al., 2016). These compounds are known to act as anticancer agents as we compared with previous literatures in PubChem databases. The CPT derivative studies and the rest of peak isolates were identified through the library of PubChem. Due to different metabolic pathways in fungal cultures it might produce both CPT and its various derivatives. In such cases, strategies should be developed to improve the production of CPT through biosynthetic pathway must be considered. Along with CPT, twelve other known compounds were obtained through ESI-MS, which was identified with databases and analyzed the *in-silico* toxic studies using TEST software. These compounds showed no toxic or less toxic in oral Rat model.

#### 3.5. In-vitro activity assessment of cancer affected cells by MTT assay

Mitochondrial synthesis of MTT assay was performed for the anti-cancerous activity of partially purified fungal crude extract containing CPT on A-549 cancer cells. The human cancer cell line of A-549 was tested in the fungal CPT concentration range of 250–31.25 µg/ml used with controls. The solvent system was used as DMSO: Methanol in the ratio of 4:1 to analyze the CPT anti-cancerous activity. CPT derivatives were cytotoxic to A-549 lung cancer cell lines (IC<sub>50</sub> 58.28 µg/ml). These results are comparable to the (IC<sub>50</sub> 51.08 µg/ml) positive control of standard CPT (Fig. 3 a & b). The fungal CPT extract showed a slightly lesser cytotoxic effect on the A-549 lung cancer cell line when compared with standard CPT at a lower concentration of IC<sub>50</sub> and it might be due to its crude nature. Similar results were obtained by (Lian et al., 2020; Venugopalan et al., 2016) on different cancer cell lines such as HEK293T, Melanoma cells, Caco-2, MCF-7, and HeLa against fungal CPT and Standard CPT. Derivatives of the anticancer molecule have a synergistic effect that leads to cytotoxicity in cancer cells (Shweta et al., 2013; Venugopalan et al., 2016). reported that various cancer cell line studies with fungal CPT effects showed evidence of a negligible difference in IC<sub>50</sub> values. The CPT derivatives involved in the inhibition of the

**Table 1**

List of Camptothecin producing endophytic fungi.

Host	Endophytic fungi	Yield	Reference
Hyphomycetes/Ascomycetes fungi			
<i>Nothapodytes foetida</i>	RJMEF001 Strain - <i>Entrophospora infrequens</i>	49.6 µg/g	Puri et al. (2005)
<i>Nothapodytes foetida</i>	<i>Nodulisporium</i> sp.,	5.5 µg/g	(Rehman et al., 2008)
<i>Camptotheca acuminata</i>	<i>Fusarium solani</i>	+	(Kusari et al., 2009)
<i>Apodytes dimidiata</i>	<i>Fusarium solani</i>	0.37 µg/g	Shweta et al. (2013)
<i>Camptotheca acuminata</i>	<i>Xylaria</i> sp., M20	5.4 µg/L	Liu et al. (2010)
<i>Miquelia dentata</i>	<i>Alternaria alternata</i>	73.9 µg/g	Shweta et al. (2013)
	<i>Fomitopsis</i> sp.,	55.49 µg/g	Shweta et al. (2013)
	<i>Phomopsis</i> sp.,	42.06 µg/g	Shweta et al. (2013)
<i>Camptotheca aquiminata</i>	<i>Aspergillus</i> sp., LY341	7.93 µg/L	Pu et al. (2013)
	<i>Trichoderma atroviride</i> LY357	197.82 µg/g	Pu et al. (2013)
<i>Nothapodytes foetida</i>	<i>Fusarium oxysporum</i> NFX06	610.1 ng/g	Musavi et al. (2014)
<i>Apodytes dimidiata</i>	<i>Fusarium solani</i> MTCC 9668	2.8 µg/L	Venugopalan and Srivastava. (2015)
<i>Nothapodytes nimmoniana</i>	<i>Fusarium oxysporum</i>	90 mg/L	Bhalkar et al. (2016)
<i>Nothapodytes nimmoniana</i>	Isolate 5 + Isolate 6	145 mg/L	Bhalkar et al. (2016)
<i>Chonemorpha fragrans</i>	<i>Fusarium solani</i> strain ATLOY-8	14.1 µg/g	Clarence et al. (2019)
Camptothecin from coelomycetous fungi from Sathyamangalam Tiger Reserve Forest (Western Ghats)			
Coelomycetes fungi			
<i>Cipadessa baccifera</i> (Roth) Miq.	<i>Guignardia vaccinii</i> sexual state of <i>Phyllosticta elongata</i> MH458897	0.747 mg/L	This is the first report

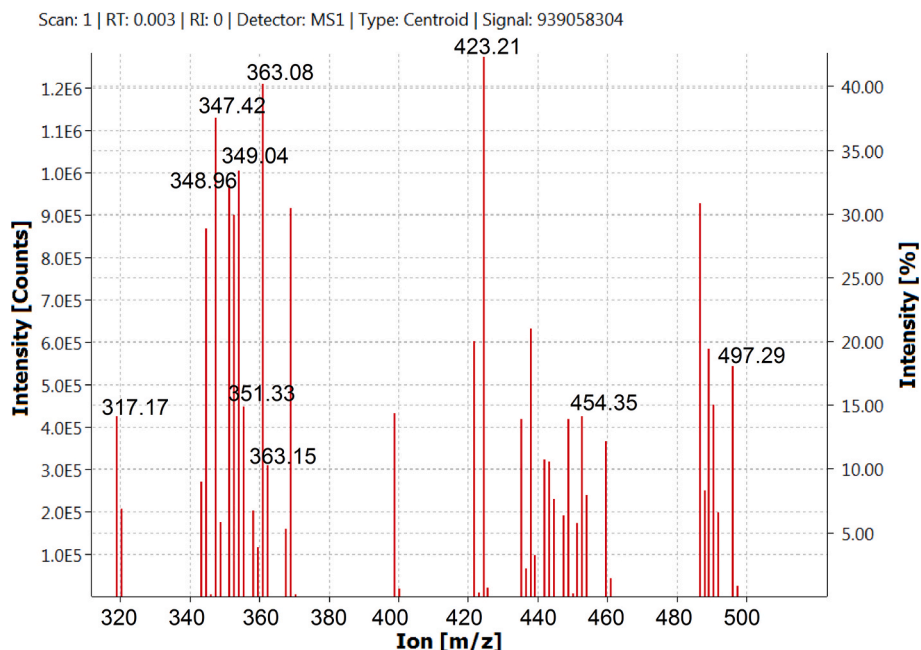


Fig. 2. Structural characterization of Electron Spray Ionization – Mass Spectrometry spectrum of Fungal CPT from *Phyllosticta elongata*.

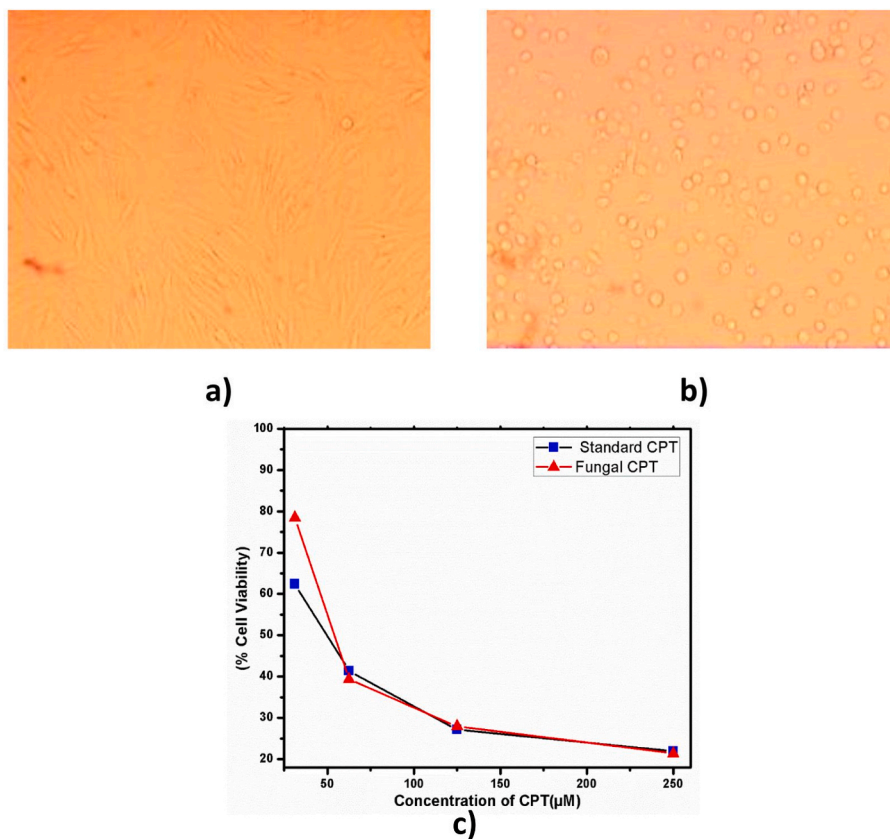


Fig. 3. (a–c) Cytotoxicity assay of a) standard CPT and b) fungal CPT against A549 Lung cancer cell line c) Effect of standard CPT and fungal CPT at varying concentrations on cell viability.

transcription process, and it could be because A-549 cancer cells with CPT derivatives react to lesser sensitivity and give cytotoxic effects to cancer cells. The fungal extracts were found to inhibit the growth of lung cancer cells of A549 at low concentrations. The toxic effect was elevated if the concentration was high, i.e., IC<sub>50</sub> is greater than its concentration

of growth of cancer cells in the human system. This cytotoxicity study revealed that fungal CPT extract was a pre-eminent inhibitor to cancerous cells. MTT assay of the cytotoxic effect of fungal CPT extract was similar to that of standard CPT at various concentrations of 250 µM, 125 µM, 62.5 µM, 31.25 µM was represented (Fig. 3 c). The percentage of

viability was tested against fungal CPT, and standard CPT showed significant cytotoxicity effect against the A549 cell line. The CPT concentrations of IC<sub>50</sub> values of both fungal CPT and standard CPT on the A549 cell line was a similar effect at 250 µM, the cell viability count indicating greater cytotoxic effect and this could be due to CPT binding effect in the cancer cell line (Puri et al., 2005). were showed similar results in the A549 cancer cell line; cell growth was terminated in IC<sub>50</sub> value at high concentration with less sensitivity. The significant number of tumor cells was inhibited by fungal CPT IC<sub>50</sub> at 58.28 µg/ml.

### 3.6. Optimization of the medium, process parameters, and its interactions

Interaction parameters of glucose, peptone, magnesium sulphate and incubation time were studied using response surface methodology to increase the CPT yield. The levels of parameter inputs were chosen on the basis of previous literatures (Bhalkar et al., 2016; Clarence et al., 2019; Musavi et al., 2015). The experimental design of CCD through RSM was generated, and it can be seen in (Table 2). A total of 28 runs were performed in random order with given variables. The response was generated as an interaction of parameters with each other. Model F-value of 84.13 indicates the model was significant, and there might be only a 0.01% chance due to noise. The fit summary for this model was observed that quadratic model terms were significant, and the sequential p-value of 0.0189. Lack of Fit F-value of 0.49 implies the Lack of Fit is not significant relative to the pure error. The lack of fit 0.6541 was a non-significant and significant value of experimental design could be considered for interaction analysis. Therefore, the optimization study was carried out with this experimental design.

#### 3.6.1. Interaction of medium parameters and validation of optimization process by RSM

RSM was used to study the kinetic growth rate of fungi that were utilizing the input parameters to increase the biomass as well as CPT yield. ANOVA test was carried out using RSM to study the interaction variables with its significance to each other. The ANOVA results of CPT response with input factors were shown here in (Table 3). The effects of

interaction parameters of (Glucose (X1) \* Peptone (X2) \* Magnesium sulphate (X3) \* Incubation time (X4)) indicates that carbon and nitrogen sources were influenced much in fungal growth and it might alter the metabolic pathway to increase the CPT yield. The interaction effects of carbon and nitrogen source in the CPT producing medium was vital to increase the biomass and metabolite concentration (Fig. 4(a–f)). The design expert trial version 12 Software was used to generate 3-D and 2-D (2D) contour plots. The 3D plots are graphical representations for the optimization of various parameters involved in most useful approach in lab-scale system. In such plots, response functions of two factors were presented while others were fixed factors in the system. The results of interactions between four independent variables and dependent variable are shown in Fig. 4(a–f). These graphs determined the optimum values of variables, as it can be seen in Fig. 4(a–f), all the 3D contour plots obtained were elliptical. Fig. 4(a–f) are positive effect on CPT yield. Contour plot of Fig. 4a showed the effect of (X4) and (X4) involved fungal biomass and CPT were steadily increased with these interdependent parameters. Fig. 4b showed CPT was not significantly affected when interactions between (X2) and (X4) at optimized conditions. When both variables were increased from –1 to 1 level, CPT was increased linearly. Plot between (X1) and (X4) showed positive effect on CPT with increase in levels of (X4) and decreased in levels of (X1), as simultaneous increase in CPT concentration (Fig. 4c). Plotted between X1 vs X3 and X2 vs X3 showed the effect of parameters involved at optimized conditions was found to increase linearly with increase in biomass concentration and CPT (Fig. 4 d and e). Use Fig Plot 4f showed the nonlinear trends observed between X1 and X2 both variables showing positive effect of stretching plot into increase yield of CPT at optimized conditions. Maximum CPT was obtained, when glucose concentration was high and biomass was high when glucose and peptone dose was high, so, the study indicates that growth of *P. elongata* mycelia directly depends on glucose and peptone but CPT yield was high when glucose was high and the peptone was optimal with respective time. These conditions were optimal with pH 5.6 at 27 °C for 14 days to achieve maximum efficiency of CPT production. The effect of each parameters was determined by F value and p value, the larger F value and smaller p value is

**Table 2**  
Experimental design for optimization of CPT producing parameters with measured and estimated response using RSM.

Run order	Dextrose g/L	Peptone g/L	Magnesium sulphate g/L	Incubation time (h)/Days	Incubation time (h)/Days	Measured actual response mg/L	Predicted response using RSM mg/L
1	10	1	0.6	336	14	0.6514	0.649
2	30	5.5	0.6	216	9	0.6483	0.6445
3	50	10	0.6	336	14	0.668	0.6656
4	30	5.5	0.1	216	9	0.6679	0.6641
5	50	10	0.1	96	4	0.1021	0.0997
6	30	5.5	0.35	216	9	0.694	0.6708
7	50	5.5	0.35	216	9	0.6408	0.637
8	10	10	0.6	96	4	0.5773	0.5749
9	30	10	0.35	216	9	0.6253	0.6215
10	50	1	0.6	336	14	0.6799	0.6833
11	10	10	0.6	336	14	0.6539	0.6573
12	10	1	0.1	336	14	0.6681	0.6715
13	30	5.5	0.35	336	14	0.6632	0.6594
14	10	1	0.1	96	4	0.488	0.4855
15	30	5.5	0.35	96	4	0.6234	0.6196
16	50	1	0.1	96	4	0.1809	0.1843
17	10	10	0.1	96	4	0.3341	0.3375
18	50	1	0.6	96	4	0.5488	0.5464
19	50	1	0.1	336	14	0.6843	0.6818
20	30	1	0.35	216	9	0.6463	0.6425
21	30	5.5	0.35	216	9	0.6577	0.6708
22	50	10	0.6	96	4	0.6071	0.6105
23	10	10	0.1	336	14	0.6699	0.6675
24	30	5.5	0.35	216	9	0.6488	0.6708
25	50	10	0.1	336	14	0.6585	0.6619
26	10	1	0.6	96	4	0.5607	0.5641
27	30	5.5	0.35	216	9	0.6599	0.6708
28	10	5.5	0.35	216	9	0.6325	0.6286



**Table 3**  
ANOVA (Cubic model - aliased) test of response surface methodology using central composite design for the optimization of CPT.

Source	Sum of Squares	Degree of Freedom	Mean Square	F - value	P - value	
Model	0.5793	22	0.0263	84.13	<0.0001	significant
A: Dextrose	0.0000	1	0.0000	0.1113	0.7522	
B: Peptone	0.0002	1	0.0002	0.7061	0.4391	
C: Magnesium sulphate	0.0002	1	0.0002	0.6119	0.4695	
D: Incubation time	0.0008	1	0.0008	2.53	0.1727	
AB	0.0004	1	0.0004	1.12	0.3385	
AC	0.0221	1	0.0221	70.65	0.0004	
BC	0.0065	1	0.0065	20.75	0.0061	
A <sup>2</sup>	0.0037	1	0.0037	11.89	0.0183	
B <sup>2</sup>	0.0039	1	0.0039	12.40	0.0169	
C <sup>2</sup>	0.0007	1	0.0007	2.24	0.1950	
D <sup>2</sup>	0.0025	1	0.0025	8.06	0.0363	
Residual	0.0016	5	0.0003			
Lack of Fit	0.0004	2	0.0002	0.4907	0.6541	not significant
Pure Error	0.0012	3	0.0004			
Cor Total	0.5809	27				
SD	0.0177		R <sup>2</sup>		0.9973	
Mean	0.5908		Adjusted R <sup>2</sup>		0.9855	
CV%	2.99		Predicted R <sup>2</sup>		0.8779	

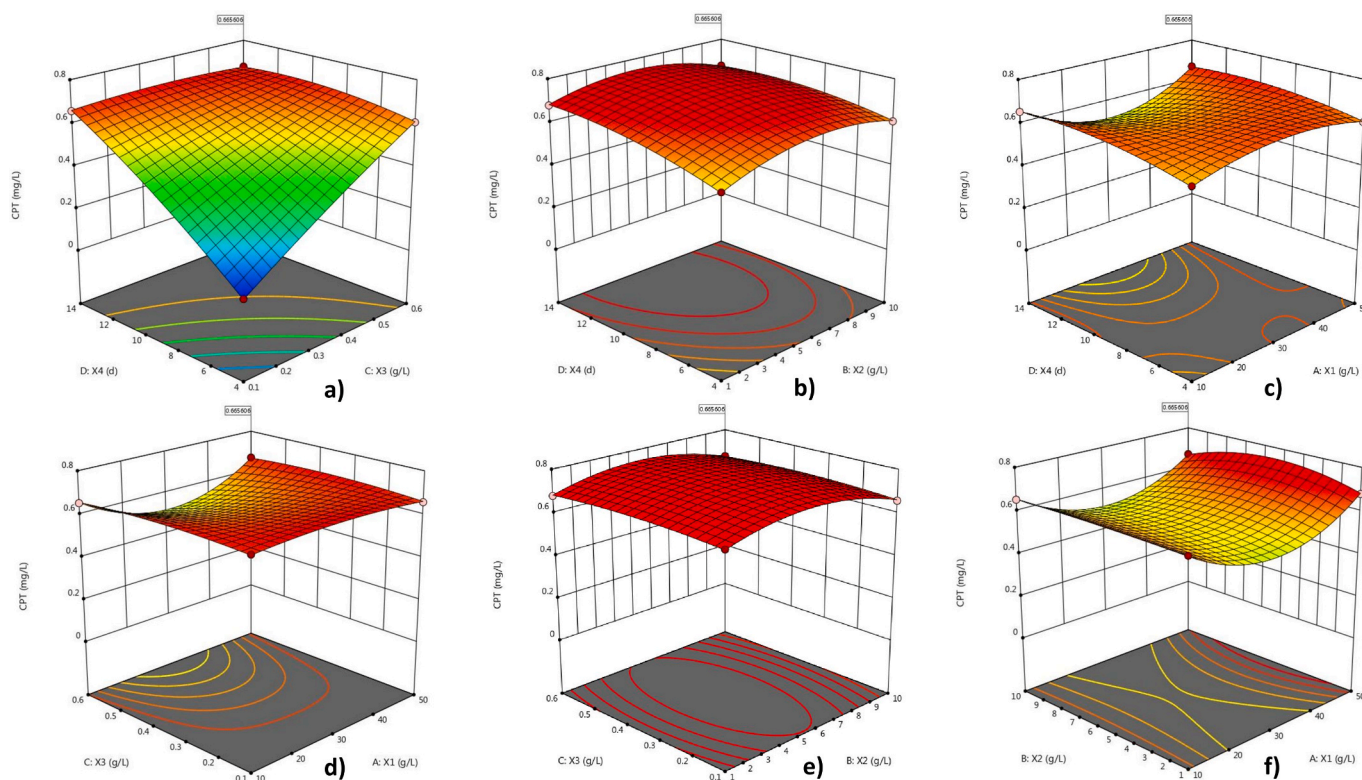


**Fig. 4.** (a–f) 3D response surface plot - Interaction between parameters to produce high amount of CPT.

more significant. As shown in (Table 3), we concluded that the independent variables of quadratic model, the interactions between glucose and peptone, peptone and magnesium sulphate, are significant because  $p < 0.05$ . P-values less than 0.0500 indicate model terms are significant. In this case AC, AD, BC, CD, A<sup>2</sup>, B<sup>2</sup>, D<sup>2</sup>, ACD, BCD, A<sup>2</sup>C, A<sup>2</sup>D are significant model terms. The p value  $> 0.05$  means that the model terms are insignificant, from (Table 3) that the interactions between glucose and

peptone, and the second order magnesium sulphate were insignificant. Values greater than 0.1000 indicate the model terms are not significant. Non-significant lack of fit was good and the model was fitted for analysis. The R<sup>2</sup> of the co-efficient determination of model was 0.9973, CV% (Co-efficient of variance), and SD (Standard Deviation) were 2.99 and 0.0177, respectively. The predicted R<sup>2</sup> of 0.8779 was in reasonable difference with less than 0.2, with an adjusted R<sup>2</sup> of 0.9855. The

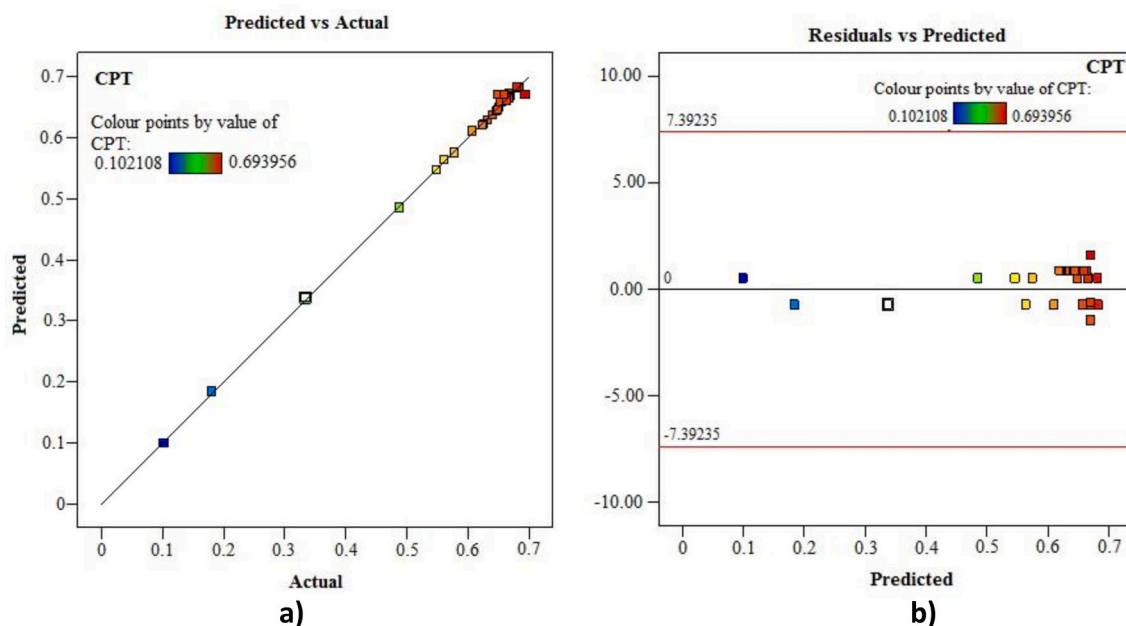


Fig. 5. (a–b) (a) Actual vs predicted values for biomass and CPT yield indicates closely to the diagonal line (b) Residual vs predicted values for biomass and CPT yield indicates closely to the diagonal line.

interaction between these variables was observed both predicted and adjusted  $R^2$  was quite significant, and the model was validated successfully (Fig. 5 a and b). The coded final polynomial equation was obtained through RSM response, and the equation was given below (Eq. (3)).

$$\begin{aligned}
 \text{CPT Response} = & 0.6708 + 0.0042 * \text{Glucose} - 0.0105 * \text{Peptone} - 0.0098 * \\
 & \text{Magnesiumsulphate} + 0.0199 * \text{Incubationtime} + 0.0047 * \text{Glucose} * \text{Peptone} + \\
 & 0.0372 * \text{Glucose} * \text{Magnesiumsulphate} + 0.0355 * \text{Glucose} * \text{Incubationtime} + \\
 & 0.0201 * \text{Peptone} * \text{Magnesiumsulphate} + 0.0078 * \text{Peptone} * \\
 & \text{Incubationtime} - 0.0760 * \text{Magnesiumsulphate} * \text{Incubationtime} - 0.0380 * \\
 & \text{Glucose}^2 - 0.0388 * \text{Peptone}^2 - 0.0165 * \text{Magnesiumsulphate}^2 - 0.0313 * \\
 & \text{Incubationtime}^2 - 0.0013 * \text{Glucose} * \text{Peptone} * \text{Magnesiumsulphate} - 0.0099 * \\
 & \text{Glucose} * \text{Peptone} * \text{Incubationtime} - 0.0324 * \text{Glucose} * \text{Magnesiumsulphate} * \\
 & \text{Incubationtime} - 0.0183 * \text{Peptone} * \text{Magnesiumsulphate} * \\
 & \text{Incubationtime} - 0.0014 \text{Glucose}^2 * \text{Peptone} + 0.0824 * \text{Glucose}^2 * \\
 & \text{Magnesiumsulphate} + 0.1010 * \text{Glucose}^2 * \text{Incubationtime} - 0.0338 * (\text{Glucose} * \\
 & \text{Peptone})^2
 \end{aligned}
 \tag{3}$$

The optimization study was carried out using estimated optimum conditions at various parameters of dextrose – 50 g L<sup>-1</sup>, peptone – 5.708 g L<sup>-1</sup>, magnesium sulphate – 0.593 g L<sup>-1</sup>, and incubation time – 14 days respectively. The experimental study revealed that, CPT yield was much higher in the optimized DEKM07 medium interacted with wild forest strain of *Phyllosticta elongata* and the CPT yield of about 0.747 mg/L. This was very close to the estimated value of 0.744 g L<sup>-1</sup> predicted by the CCD design of RSM (Musavi et al., 2015). reported that 610.09 ng/g of CPT release of actual response and CPT of predicted response 628.08 ng/g from *Fusarium oxysporum* NFX06 with 15.91 g L<sup>-1</sup> of biomass. However, in our study we have used low peptone dosage of 5.78 g L<sup>-1</sup> for CPT optimization due to cost limits of peptone dosage and also to achieve maximum biomass and CPT. Hence, the interaction of parameters with the fungus was optimal to produce the maximum yield of CPT. A good correlation between estimated and actual response confirmed that the model fitted well, and the experimental study perfectly reflects the estimated study design by RSM. Endophytic fungus, *Phyllosticta elongata* could act as potential source of Camptothecin production in host as well as in lab scale environment. It is therefore assumed that these endophytes played a vital role in the plants in forest ecosystem. For instance, Table 1 showed that many secondary metabolites were

produced from endophytic fungi from different hosts. This type of potential wild strains is highly present in biotic environment of core regions of forest (Strobel, 2002). These metabolites are major source will be used in research/pharmacological sector to develop a new molecule to overcome the pandemic situations. Forest ecosystem should be preserved both biotic and abiotic factors need to be protected at optimal way with minimal forest fires and pollution less environment. In the present study, there are some limitations which we faced during the lab-scale experiments i.e., the amounts of inoculum spores were optimized to increase biomass and CPT yield. Incubation time is also an additional critical factor for increasing yield. If we increase the incubation time, there will be loss of product/product yield due to over exploitation of fungal biomass in flasks it leads to utilize the CPT product for survival of fungal growth. The biosynthetic mechanism of CPT is another difficult task due to biosynthetic pathways in plants and endophytic fungi. CPT production capacity was reduced following repeated subcultures due to lab-scale and pilot-scale production. Endophytes acts as keystone species in terrestrial ecosystem, these are relatively less explored microbes from the natural environment. Research on fungal compounds for cancer reduction in recent decades has made significant progress in terms of drug delivery and cancer immunotherapy (How et al., 2021). Detection of cancer at early stage using circulating miRNA biomarkers is desirable as these miRNAs (MiR-21) are present in the fluids body and may be achieved with minimally invasive or non-invasive methods. MiR-21 expression is upregulated in non-small cell lung cancer patient (Shin Low et al., 2020). Our further studies will enhance the abiotic factors under pilot scale to increase the product yield, to overcome the major limitations which we discussed earlier and also with cancer detection biomarkers like MiR-21 expression. So that, we can produce economically suitable anticancer drugs serves to this society. The present study provides comprehensive data of endophytic fungal diversity present in particular ecosystem and it secondary metabolites recovery under lab scale environment.

#### 4. Conclusion

The results obtained in the study concluded the potential strain *Phyllosticta elongata* isolated from Sathyamangalam Tiger Reserve Forest has immense potential to utilize it as a source for the production of CPT.

DEKM07 was identified as a suitable medium for the production of CPT and the RSM results showed the optimum conditions for the maximum yield of fungal biomass and CPT. This is the first report on CPT from *Phyllosticta elongata* isolated from *Cipadessa baccifera* with a maximum yield of 0.747 mg/L. Our findings support the novel lifesaving anticancer drug from endophytic fungus in forest ecosystem concludes effective utilization of keystone species will safeguard the humans and forest ecosystem.

## Declaration of competing interest

The authors declare that they have no known competing financial interests or personal relationships that could have appeared to influence the work reported in this paper.

## Acknowledgements

Financial support for this work was provided by the Directorate of Extramural Research & Intellectual Property Rights (ER & IPR) Defense Research Development Organization, Ministry of Defence, Government of India (Ref. No. IP/ER/1104597/M/01M1493). The authors are grateful to Divisional Forest Officer and Field Directors of the Tamil Nadu Forest Department, Sathyamangalam, and Haasanur Division, Erode District, Tamil Nadu, India (D/5589/2015 Dated on March 14, 2016). The authors extend their acknowledgment to the National Biodiversity Authority, Chennai. The authors are thankful to the Botanical Survey of India, Southern Division, Coimbatore, India, for identifying the medicinal plants. Authors express their gratitude to CATERS, Central Leather Research Institute, Chennai, for ESI-MS facilities provided, and Gujarat State Biotechnology Mission, Gandhi Nagar, Gujarat India, for their help in the 18SrDNA sequencing. Sincere thanks to the management of Bannari Amman Institute of Technology, Sathyamangalam, for providing the necessary facilities.

## Appendix A. Supplementary data

Supplementary data to this article can be found online at <https://doi.org/10.1016/j.envres.2021.111564>.

## References

- Amna, T., Amina, M., Sharma, P.R., Puri, S.C., Al-Youssef, H.M., Al-Taweel, A.M., Qazi, G.N., 2012. Effect of precursors feeding and media manipulation on production of novel anticancer pro-drug camptothecin from endophytic fungus. *Braz. J. Microbiol.* 43, 1476–1489. <https://doi.org/10.1590/S1517-83822012000400032>.
- Arjunan, V., Saravanan, I., Ravindran, P., Mohan, S., 2009. Ab initio, density functional theory and structural studies of 4-amino-2-methylquinoline. *Spectrochim. Acta Part A Mol. Biomol. Spectrosc.* 74, 375–384. <https://doi.org/10.1016/j.saa.2009.06.028>.
- Bellamy, L.J., 1975. *The Infrared Spectra of Complex Molecules*, third ed. Wiley, New York, p. 433.
- Bhalkar, B.N., Patil, S.M., Govindwar, S.P., 2016. Camptothecin production by mixed fermentation of two endophytic fungi from *Nothapodytes nimmoniana*. *Fungal Biol.* 120, 873–883. <https://doi.org/10.1016/j.funbio.2016.04.003>.
- Bray, F., Ferlay, J., Soerjomataram, I., Siegel, R.L., Torre, L.A., Jemal, A., 2018. Global cancer statistics 2018: GLOBOCAN estimates of incidence and mortality worldwide for 36 cancers in 185 countries. *CA. Cancer J. Clin.* 68, 394–424. <https://doi.org/10.3322/caac.21492>.
- Busby, P.E., Ridout, M., Newcombe, G., 2016. Fungal endophytes: modifiers of plant disease. *Plant Mol. Biol.* 90, 645–655. <https://doi.org/10.1007/s11103-015-0412-0>.
- Calvo, A.M., Wilson, R.A., Bok, J.W., Keller, N.P., 2002. Relationship between secondary metabolism and fungal development. *Microbiol. Mol. Biol. Rev.* 66, 447–459. <https://doi.org/10.1128/mmr.66.3.447-459.2002>.
- Chai, W.S., Cheah, K.H., Meng, H., Li, G., 2019. Experimental and analytical study on electrolytic decomposition of HAN-water solution using graphite electrodes. *J. Mol. Liq.* 293, 111496. <https://doi.org/10.1016/j.molliq.2019.111496>.
- Chen, Y., Sun, L.T., Yang, H.X., Li, Z.H., Liu, J.K., Ai, H.L., Wang, G.K., Feng, T., 2020. Desipones and diaryl ethers from potato endophytic fungus *Boeremia exigua*. *Fitoterapia* 141, 104483. <https://doi.org/10.1016/j.fitote.2020.104483>.
- Clarance, P., Khusro, A., Lalitha, J., Sales, J., Paul, A., 2019. Optimization of camptothecin production and biomass yield from endophytic fungus *Fusarium solani* strain ATLOY-8. *J. Appl. Pharmaceut. Sci.* 9, 35–46. <https://doi.org/10.7324/japs.2019.91005>.
- Dhakshinamoorthy, M., Kilavan Packiam, K., Kumar, P.S., Saravanakumar, T., 2021. Endophytic fungus *Diaporthe caatingaensis* MT192326 from *Buchanania axillaris*: an indicator to produce biocontrol agents in plant protection. *Environ. Res.* 197, 111147. <https://doi.org/10.1016/j.envres.2021.111147>.
- Govinda Rajulu, M.B., Thirunavukkarasu, N., Babu, A.G., Aggarwal, A., Suryanarayanan, T.S., Reddy, M.S., 2013. Endophytic xylariaceae from the forests of Western Ghats, southern India: distribution and biological activities. *Mycology* 4, 29–37. <https://doi.org/10.1080/21501203.2013.776648>.
- Hertzberg, R.P., Caranfa, M.J., Hecht, S.M., 1989. On the mechanism of topoisomerase I inhibition by camptothecin: evidence for binding to an enzyme-DNA complex. *Biochemistry* 28, 4629–4638. <https://doi.org/10.1021/bi00437a018>.
- How, C.W., Ong, Y.S., Low, S.S., Pandey, A., Show, P.L., Foo, J.B., 2021. How far have we explored fungi to fight cancer? *Semin. Canc. Biol.* <https://doi.org/10.1016/j.semcancer.2021.03.009>.
- Jiang, Z., Zhang, Z., Cui, G., Sun, Z., Song, G., Liu, Y., Zhong, G., 2018. DNA Topoisomerase I structure-BASED design, synthesis, activity evaluation and molecular simulations study of new 7-amide camptothecin derivatives against *Spodoptera frugiperda*. *Front. Chem.* 6, 1–14. <https://doi.org/10.3389/fchem.2018.00456>.
- Joseph, B.L., Herbert F. S., Cooks, R.G., et al., 1987. *Introduction to Organic Spectroscopy*. Macmillan Publication, NY, pp. 174–177.
- Kai, G., Wu, C., Gen, L., Zhang, L., Cui, L., Ni, X., 2015. Biosynthesis and biotechnological production of anti-cancer drug Camptothecin. *Phytochem. Rev.* <https://doi.org/10.1007/s11101-015-9405-5>.
- Kathiravan, G., Sri Raman, V., 2010. In vitro Taxol production, by *Pestalotiopsis breviseta* - a first report. *Fitoterapia* 81, 557–564. <https://doi.org/10.1016/j.fitote.2010.01.021>.
- Kumar, D.S.S., Hyde, K.D., 2004. Biodiversity and tissue-recurrence of endophytic fungi in *Tripterygium wilfordii*. *Fungal Divers.* 17, 69–90.
- Kumar, S., Stecher, G., Li, M., Knyaz, C., Tamura, K., 2018. MEGA X: molecular evolutionary genetics analysis across computing platforms. *Mol. Biol. Evol.* 35, 1547–1549. <https://doi.org/10.1093/molbev/msy096>.
- Kumaran, R.S., Muthumary, J., Hur, B.K., 2009. Isolation and identification of an anticancer drug, taxol from *Phyllosticta tabernaemontanae*, a leaf spot fungus of an angiosperm, *Wrightia tinctoria*. *J. Microbiol.* 47, 40–49. <https://doi.org/10.1007/s12275-008-0127-x>.
- Lian, C., Cao, S., Zeng, W., Li, Y., Su, J., Li, J., Zhao, S., Wu, L., Tao, J., Zhou, J., Chen, X., Peng, C., 2020. RJT-101, a novel camptothecin derivative, is highly effective in the treatment of melanoma through DNA damage by targeting topoisomerase I. *Biochem. Pharmacol.* 171 <https://doi.org/10.1016/j.bcp.2019.113716>.
- Liu, K., Ding, X., Deng, B., Chen, W., 2010. 10-Hydroxycamptothecin produced by a new endophytic *Xylaria* sp., M20, from *Camptotheca acuminata*. *Biotechnol. Lett.* 32, 689–693. <https://doi.org/10.1007/s10259-010-0201-4>.
- Liu, Q., Luyten, W., Pellens, K., Wang, Y., Wang, W., Thevissen, K., Liang, Q., Cammue, B.P.A., Schoofs, L., Luo, G., 2012. Antifungal activity in plants from Chinese traditional and folk medicine. *J. Ethnopharmacol.* 143, 772–778. <https://doi.org/10.1016/j.jep.2012.06.019>.
- Musavi, S.F., Balakrishnan, R.M., 2014. A study on the antimicrobial potentials of an endophytic fungus *Fusarium oxysporum* NFX 06. *J. Med. Bioeng.* 3, 162–166. <https://doi.org/10.12720/jomb.3.3.162-166>.
- Musavi, S.F., Dhavale, A., Balakrishnan, R.M., 2015. Optimization and kinetic modeling of cell-associated camptothecin production from an endophytic *Fusarium oxysporum* NFX06. *Prep. Biochem. Biotechnol.* 45, 158–172. <https://doi.org/10.1080/10826068.2014.907177>.
- Nagraj, T.R., Jones, G.M., Kendrick, B., 1972. *Genera coelomycetorum IV Pseudorobillardia* gen.nov. A generic segregate of *Robillarda* Sacc. *Can. J. Bot.* 50, 861–867.
- Nat, R., Chem, P., Raveendran, V.V., 2015. Camptothecin-discovery, clinical perspectives and Biotechnology. *Nat. Prod. Chem. Res.* 3 <https://doi.org/10.4172/2329-6836.1000175>.
- Ning, J., Di, Y.T., Fang, X., He, H.P., Wang, Y.Y., Li, Y., Li, S.L., Hao, X.J., 2010a. Limonoids from the leaves of *Cipadessa baccifera*. *J. Nat. Prod.* 73, 1327–1331. <https://doi.org/10.1021/np900852d>.
- Ning, J., Di, Y.T., Wang, Y.Y., He, H.P., Fang, X., Li, Y., Li, S.L., Hao, X.J., 2010b. Cytotoxic activity of trjugin-type limonoids from *Cipadessa baccifera*. *Planta Med.* 76, 1907–1910. <https://doi.org/10.1055/s-0030-1249979>.
- Nomila Merlin, J., Nimal Christudas, I.V.S., Praveen Kumar, P., Agastian, P., 2013. Optimization of growth and bioactive metabolite production: *Fusarium solani*. *Asian J. Pharmaceut. Clin. Res.* 6, 98–103.
- Patil, A., Patil, S., Mahure, S., Kale, A., 2014. UV, FTIR, HPLC confirmation of camptothecin an anticancer metabolite from Bark extract of *Nothapodytes nimmoniana* (J. Graham). *Am. J. Ethnomed.*
- Pommier, Y., 2006. Topoisomerase I inhibitors: camptothecins and beyond. In: *Nature Reviews Cancer*, pp. 789–802. <https://doi.org/10.1038/nrc1977>.
- Pu, X., Qu, X., Chen, F., Bao, J., Zhang, G., Luo, Y., 2013. Camptothecin-producing endophytic fungus *Trichoderma atroviride* LY357: isolation, identification, and fermentation conditions optimization for camptothecin production. *Appl. Microbiol. Biotechnol.* 97, 9365–9375. <https://doi.org/10.1007/s00253-013-5163-8>.
- Puri, S.G., Verma, V., Amna, T., Qazi, G.N., Spittler, M., 2005. An endophytic fungus from *Nothapodytes foetida* that produces camptothecin. *J. Nat. Prod.* 68, 1717–1719. <https://doi.org/10.1021/np050280z>.
- Ramkumar, G., Karthi, S., Muthusamy, R., Natarajan, D., Shivakumar, M.S., 2015. Antidotal and smoke toxicity of *Cipadessa baccifera* (Roth) plant extracts against *Anopheles stephensi*, *Aedes aegypti*, and *Culex quinquefasciatus*. *Parasitol. Res.* 114, 167–173. <https://doi.org/10.1007/s00436-014-4173-5>.

- Reddy, A.M., Babu, M.V.S., Rao, R.R., 2019. Ethnobotanical study of traditional herbal plants used by local people of Seshachalam Biosphere Reserve in Eastern Ghats, India. *Herba Pol.* 65, 40–54. <https://doi.org/10.2478/hepo-2019-0006>.
- Reddy, M.S., Murali, T.S., Suryanarayanan, T.S., Govinda Rajulu, M.B., Thirunavukkarasu, N., 2016. *Pestalotiopsis* species occur as generalist endophytes in trees of Western Ghats forests of southern India. *Fungal Ecol* 24, 70–75. <https://doi.org/10.1016/j.funeco.2016.09.002>.
- Rodgers, K.M., Udesky, J.O., Rudel, R.A., Brody, J.G., 2018. Environmental chemicals and breast cancer: an updated review of epidemiological literature informed by biological mechanisms. *Environ. Res.* 160, 152–182. <https://doi.org/10.1016/j.envres.2017.08.045>.
- Sajan, D., Hubert Joe, I., Jayakumar, V.S., 2006. NIR-FT Raman, FT-IR and surface-enhanced Raman scattering spectra of organic nonlinear optic material: p-hydroxy acetophenone. *J. Raman Spectrosc.* 37, 508–519. <https://doi.org/10.1002/jrs.1424>.
- Shin Low, S., Pan, Y., Ji, D., Li, Y., Lu, Y., He, Y., Chen, Q., Liu, Q., 2020. Smartphone-based portable electrochemical biosensing system for detection of circulating microRNA-21 in saliva as a proof-of-concept. *Sensor. Actuator. B Chem.* 308, 127718. <https://doi.org/10.1016/j.snb.2020.127718>.
- Shweta, S., Gurumurthy, B.R., Ravikanth, G., Ramanan, U.S., Shivanna, M.B., 2013. Endophytic fungi from *Miquelia dentata* Bedd., produce the anti-cancer alkaloid, camptothecine. *Phytomedicine* 20, 337–342. <https://doi.org/10.1016/j.phymed.2012.11.015>.
- Silverstein, R.M., Bassler, C., Morill, T.C., 1991. *Spectrometric Identification of Organic Compounds*, fifth ed., vol. 39. John Wiley & Sons, p. 546.
- Socrates, G., 2001. *Infrared Raman Characteristic Group Frequencies Tables and Charts*, third ed. Wiley, Chichester.
- Subban, K., Subramani, R., Madambakkam Srinivasan, V.P., Johnpaul, M., Chelliah, J., 2019. Salicylic acid as an effective elicitor for improved taxol production in endophytic fungus *Pestalotiopsis microspora*. *PLoS One* 14, 1–17. <https://doi.org/10.1371/journal.pone.0212736>.
- Suryanarayanan, T.S., Murali, T.S., Thirunavukkarasu, N., Govinda Rajulu, M.B., Venkatesan, G., Sukumar, R., 2011. Endophytic fungal communities in woody perennials of three tropical forest types of the Western Ghats, southern India. *Biodivers. Conserv.* 20, 913–928. <https://doi.org/10.1007/s10531-011-0004-5>.
- Sutton, B.C., 1980. *The Coelomycetes*. CAB International Mycological Institute, Kew.
- Strobel, G.A., 2002. Microbial gifts from rain forests I. *J. Indian Dent. Assoc.* 24, 14–20. <https://doi.org/10.1080/07060660109506965>.
- Téllez Tovar, S.S., Rodríguez Susa, M., 2020. Cancer risk assessment from exposure to trihalomethanes in showers by inhalation. *Environ. Res.* 110401 <https://doi.org/10.1016/j.envres.2020.110401>.
- Venugopalan, A., Potunuru, U.R., Dixit, M., Srivastava, S., 2016. Effect of fermentation parameters, elicitors and precursors on camptothecin production from the endophyte *Fusarium solani*. *Bioresour. Technol.* 206, 104–111. <https://doi.org/10.1016/j.biortech.2016.01.079>.
- Venugopalan, A., Srivastava, S., 2015. Enhanced camptothecin production by ethanol addition in the suspension culture of the endophyte *Fusarium solani*. *Bioresour. Technol.* 188, 251–257. <https://doi.org/10.1016/j.biortech.2014.12.106>.
- Wang, X., Wang, C., Sun, Y.T., Sun, C.Z., Zhang, Y., Wang, X.H., Zhao, K., 2015. Taxol produced from endophytic fungi induces apoptosis in human breast, cervical and ovarian cancer cells. *Asian Pac. J. Cancer Prev. APJCP* 16, 125–131. <https://doi.org/10.7314/APJCP.2015.16.1.125>.
- Wikee, S., Lombard, L., Crous, P.W., Nakashima, C., Motohashi, K., Chukeatirote, E., Alias, S.A., McKenzie, E.H.C., Hyde, K.D., 2013. *Phyllosticta capitalensis*, a widespread endophyte of plants. *Fungal Divers.* 60, 91–105. <https://doi.org/10.1007/s13225-013-0235-8>.
- Wulandari, N.F., 2013. A modern account of the genus *Phyllosticta*. *Plant Pathol. Quar.* 3, 145–159. <https://doi.org/10.5943/ppq/3/2/4>.
- Yang, Y., Pu, X., Qu, X., Chen, F., Zhang, G., Luo, Y., 2017. Enhanced production of camptothecin and biological preparation of N 1-acetylkynuramine in *Camptotheca acuminata* cell suspension cultures. *Appl. Microbiol. Biotechnol.* 101, 4053–4062. <https://doi.org/10.1007/s00253-017-8153-4>.